THE JOURNAL OF BIOLOGICAL CHEMISTRY VOL. 287, NO. 27, pp. 22701–22708, June 29, 2012

Constitutive Activity of TRPML2 and TRPML3 Channels *versus* Activation by Low Extracellular Sodium and Small Molecules*

Received for publication, April 5, 2012, and in revised form, May 3, 2012 Published, JBC Papers in Press, May 9, 2012, DOI 10.1074/jbc.M112.368876

Christian Grimm[‡1], **Simone Jörs**[§2], **Zhaohua Guo**[§], **Alexander G. Obukhov**[¶], **and Stefan Heller**[§]

From the [‡]*Department of Pharmacy, Center for Drug Research, and Center for Integrated Protein Science Munich (CIPSM), Ludwig-Maximilians-Universität München, D-80802 München, Germany, the* [§]*Departments of Otolaryngology (Head and Neck Surgery) and Molecular and Cellular Physiology, Stanford University School of Medicine, Stanford, California 94305, and the* [¶]*Department of Cellular and Integrative Physiology, Indiana University School of Medicine, Indiana University-Purdue University Indianapolis (IUPUI), Indianapolis, Indiana 46202*

Background: Physiological function(s) and activation mechanism(s) of TRPML2 and TRPML3 channels are largely unknown.
Results: TRPML2 and TRPML3 channels are activated by different small chemical compounds and low extracellular sodium. Mutations in the first and second extracellular loops render TRPML3 constitutively active in high extracellular sodium.
Conclusion: TRPML2 and TRPML3 display similar activation mechanisms.
Significance: Novel insights into TRPML2 and TRPML3 activation are provided.

The transient receptor potential channels TRPML2 and TRPML3 (MCOLN2 and MCOLN3) are nonselective cation channels. They are widely expressed in mammals. However, little is known about their physiological function(s) and activation mechanism(s). TRPML3 can be activated or rather de-inhibited by exposing it first to sodium-free extracellular solution and subsequently to high extracellular sodium. TRPML3 can also be activated by a variety of small chemical compounds identified in a high throughput screen and is inhibited by low pH. Furthermore, it was found that TRPML3 is constitutively active in low or no sodium-containing extracellular solution. This constitutive activity is independent of the intracellular presence of sodium, and whole-cell current densities are similar with pipette solutions containing cesium, potassium, or sodium. Here, we present mutagenesis data generated based on the hypothesis that negatively charged amino acids in the extracellular loops of TRPML3 may interfere with the observed sodium inhibition. We systematically mutated negatively charged amino acids in the first and second extracellular loops and found that mutating Glu-361 in the second loop has a significant impact on the sodium-mediated block of TRPML3. We further demonstrate that the TRPML3-related cation channel TRPML2 is also activated by lowering the extracellular sodium concentration as well as by a subset of small chemical compounds that were previously identified as activators of TRPML3, thus confirming the functional activity of TRPML2 at the plasma membrane and suggesting similar gating mechanisms for both TRPML channels.

TRPML2 and TRPML3 channels are expressed in a large variety of tissues and organs, including the lung, liver, kidney, colon, thymus, testis, olfactory bulb, skin, and inner ear (1). In the inner ear, TRPML3 expression has been demonstrated for the stria vascularis of the cochlea, the organ of Corti sensory hair cells, and the utricle (1–7). In inner ear hair cells, endogenous TRPML3 was found in intracellular vesicles in the subcuticular region and the pericuticular necklace. Lower levels of TRPML3 were reportedly detectable at the plasma membrane of hair cell stereocilia (4). Hair cell bundles or stereocilia protrude into the scala media of the cochlea, which is a cochlear compartment that is filled with endolymph, an extracellular fluid low in sodium and high in potassium. We have reported previously that in the presence of low sodium bath solution (LSS),[3] TRPML3-expressing HEK293 cells showed a robust constitutively active inwardly rectifying current that was not detectable when the cells were kept in standard bath solution (SBS) containing high sodium (1). Extracellular solution containing either high potassium or high lithium as the sole cation (at 150 mM) likewise evoked currents of comparable sizes in wild-type TRPML3-expressing HEK293 cells (1). Extracellular solution containing 150 mM cesium was found to result in significantly smaller inward currents, whereas no currents were detected with the organic monovalent cation *N*-methyl-D-glucamine (150 mM). To determine whether changes in the intracellular ionic composition interfere with the activity of TRPML3, the cesium-containing pipette solution was replaced with solutions containing either 150 mM K^+ or 150 mM Na^+. In contrast to high extracellular sodium, high intracellular sodium did not block TRPML3 activity (1). These results are consistent with the finding that TRPML3 activity depends on the extracellular Na^+ concentration, as suggested previously by Kim *et al.* (8–10). Kim *et al.* (8–10) found that TRPML3 can be rendered active by exposing it initially to sodium-free extracellular solution containing 150 mM *N*-methyl-D-glucamine, followed by rapid sodium re-addition.

* This work was supported, in whole or in part, by National Institutes of Health Grants DC004563, MH083077, and P30 DC010363.
[1] To whom correspondence should be addressed. Tel.: 49-89-2180-77320; E-mail: chgrph@cup.uni-muenchen.de.
[2] Present address: II. Medizinische Klinik (Gastroenterology), Klinikum Rechts der Isar, Technische Universität München, München, Germany.

[3] The abbreviations used are: LSS, low sodium bath solution; SBS, standard bath solution; SID, PubChem substance accession identifier; TMD, transmembrane domain; TRP, transient receptor potential.

Furthermore, TRPML3 was shown to be pH-regulated (9) and activated by different small chemical compounds such as 5-mesityl-3-oxa-4-azatricyclo[5.2.1.0~2,6~]dec-4-ene (SN-2, PubChem substance accession identifier (SID) 22411609), 5-chloro-*N*-(2-piperidin-1-ylphenyl)thiophene-2-sulfonamide (SF-22, SID 14746905), and 1-(4-ethoxynaphthalen-1-yl)sulfonylazepane (SF-31, SID 14722627), which were identified in a high throughput screen (1, 11). Between the activation by LSS and the activation by different chemical stimuli, a strong synergistic effect was observed, which can result in >10-fold increases in TRPML3 current densities compared with LSS or compound in SBS alone (1).

Two different recently described constitutively active mutant TRPML3 isoforms, the deafness-causing A419P or varitint-waddler mutant isoform Va and the H283A mutant isoform, appear to be sodium-insensitive, *i.e.* high extracellular sodium does not block channel activity (2, 8–9, 12–14). However, the underlying mechanisms appear to be different from each other. In the case of A419P, which is located in the fifth transmembrane domain (TMD5), the pore structure may be directly affected. His-283 is located in the first extracellular loop, and in contrast to A419P (14), the H283A mutant is also insensitive to low extracellular pH (9). It has been suggested that this mutation causes a long-range conformational change affecting the pore loop. The first extracellular loop of TRPML channels is unusually long compared with the ones found in other transient receptor potential (TRP) channels and may indeed have unique functional properties, possibly including regulation of channel gating.

Here, we conducted a systematic site-directed mutagenesis screen based on the hypothesis that negatively charged amino acids in the extracellular loops of TRPML3 may interfere with the observed sodium block. We mutated individual negatively charged amino acids in the first and second extracellular loops and found that Glu-361 in the second loop is essential for the sodium-mediated block of TRPML3 and that mutating Glu-361 to alanine causes strongly increased channel activity in high sodium-containing SBS. We further demonstrate that TRPML2 shows increased channel activity in low extracellular sodium and is activated by a set of small chemical compounds shown before to activate TRPML3 (1), thus confirming that TRPML2 is functionally active at the plasma membrane (15) and further suggesting similar gating mechanisms for both TRPML2 and TRPML3.

EXPERIMENTAL PROCEDURES

Plasmid Constructs and Cell Lines—For calcium imaging and electrophysiological experiments in HEK293 cells, wild-type and mutant mouse TRPML3 (NM_134160), mouse TRPML2 (NM_001005846), and human TRPML1 (NM_020533) were used. All wild-type and mutant TRPML isoforms were C-terminally tagged YFP versions. For functional studies, constructs were transiently expressed in HEK293 cells (1 μg of DNA/10-cm dish with four to five glass coverslips each) using GeneJammer (Stratagene) and measured 24–48 h after transfection.

Calcium Imaging and Patch Clamp Electrophysiology—Measurements of $[Ca^{2+}]_i$ with the fluorescent indicator fura-2 AM (Invitrogen) were performed using a monochromator-based imaging system (iMIC platform and Polychrome V monochromator, TILL Photonics). HEK293 cells were loaded with 4 μM fura-2 AM in SBS containing 138 mM NaCl, 6 mM KCl, 2 mM $MgCl_2$, 2 mM $CaCl_2$, 10 mM HEPES, and 5.5 mM D-glucose (adjusted to pH 7.4 with NaOH). HEK293 cells were maintained in Earle's minimum essential medium (Invitrogen) supplemented with 10% fetal bovine serum (Invitrogen), 100 μg/ml penicillin, 100 μg/ml streptomycin under a 5% CO_2 atmosphere at 37 °C. For fluorescence measurements, cells were plated onto glass coverslips. Calcium imaging experiments were performed as described previously (1, 12, 13). Basal calcium levels shown in Fig. 1*C* are average calcium levels of experiments shown in Fig. 1*B* after subtraction of average calcium levels of non-transfected control cells (at least three per experiment).

Whole-cell currents were recorded with an Alembic Instruments VE-2 amplifier and acquired with JClamp software. The SBS used for patch clamp recordings contained 138 mM NaCl, 5.4 mM KCl, 2 mM $MgCl_2$, 2 mM $CaCl_2$, 10 mM HEPES, and 10 mM D-glucose (adjusted to pH 7.4 with NaOH). The LSS contained 150 mM KCl, 2 mM NaCl, 0.25 mM $CaCl_2$, 10 mM HEPES, and 10 mM D-glucose (adjusted to pH 7.4 with KOH). The pipette solution contained 140 mM CsCl, 10 mM HEPES, 3 mM NaATP, 1 mM 1,2-bis(*o*-aminophenoxy)ethane-*N*,*N*,*N*′,*N*′-tetraacetic acid, and 2 mM $MgCl_2$ (adjusted to pH 7.2). All experiments were performed at room temperature.

Site-directed Mutagenesis—All TRP channel mutants were generated from wild-type cDNA templates using the QuikChange site-directed mutagenesis kit (Stratagene). All mutants were verified by sequencing both strands entirely.

Laser Scanning Microscopy—Transfected HEK293 cells were analyzed 24–48 h post-transfection. The cells were washed once with PBS and analyzed in SBS using a Zeiss LSM 510 confocal microscope.

Compounds—Detailed information for all compounds is available at the PubChem Project (pubchem.ncbi.nlm.nih.gov) by conducting queries with the PubChem SID. For this study, compounds SF-21 (SID 24801657) and SF-41 (SID 24787221) were purchased from Asinex Ltd. Compound SF-81 (SID 14733059) was purchased from Key Organics. Stock solutions of the compounds were prepared at 10 mM in Me_2SO and were stored in small aliquots at −80 °C.

RESULTS

Extracellular Loop Scan Reveals Constitutive Activity of TRPML3 Alanine Mutants—On the basis of the hypothesis that one or more negatively charged amino acids in the extracellular loops may be involved in the observed inhibitory effect of high extracellular sodium on TRPML3 activity, we performed a systematic mutagenesis scan. The first extracellular loop between TMD1 and TMD2 contains 28 negatively charged residues. The second, much smaller extracellular loop between TMD3 and TMD4 contains two negatively charged amino acids (Glu-361 and Asp-371).

In an initial step, we generated the following deletion mutants: Δ90–277, Δ100–E268, Δ120–D248, ΔD173–E192, and ΔE180–E184 (Fig. 1*A*). On the one hand, this was done with the goal to find out whether a shorter first extracellular

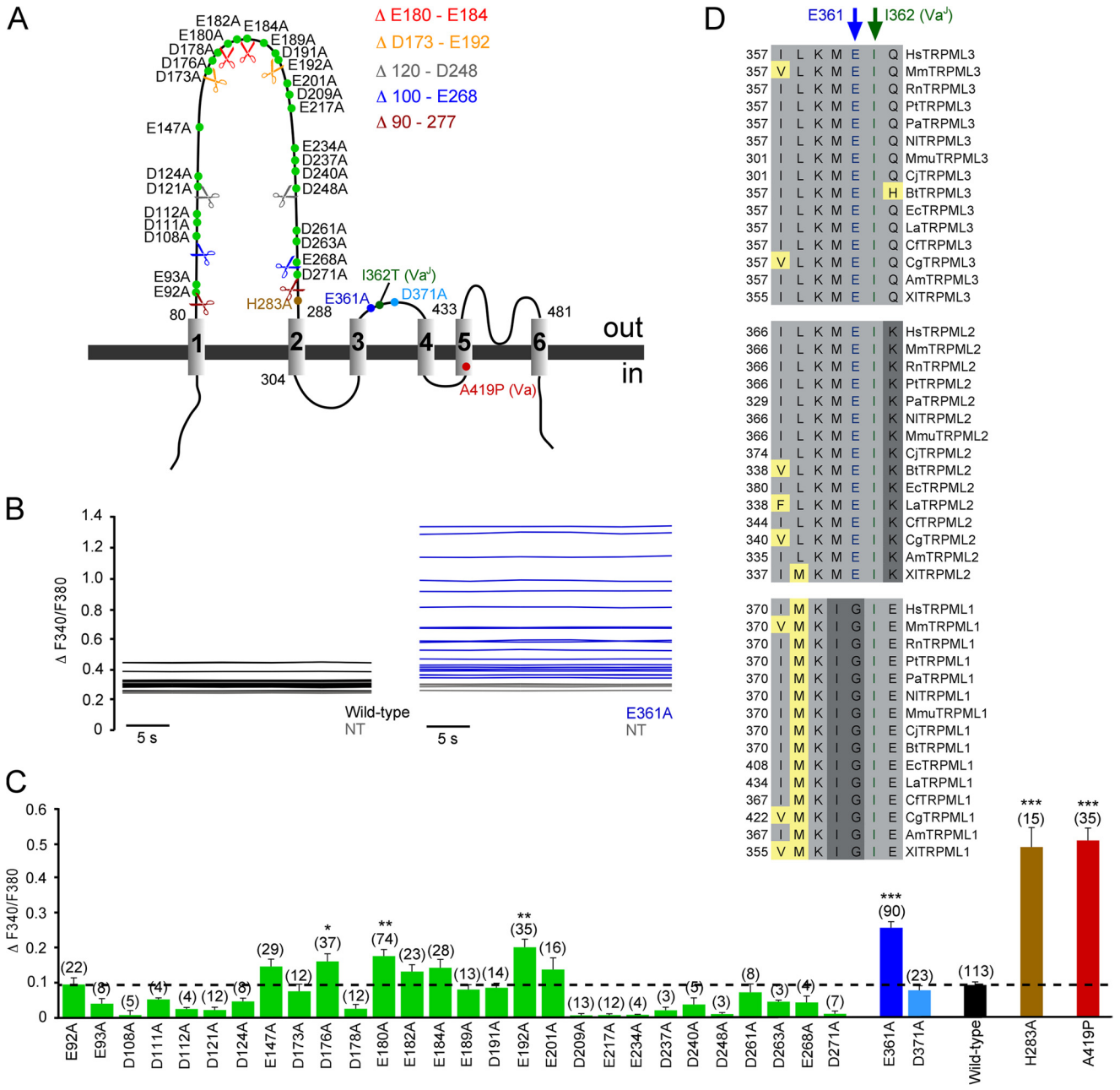

FIGURE 1. **Extracellular loop mutation increases TRPML3 open probability in high extracellular sodium.** *A*, schematic displaying the estimated positions of all negatively charged amino acids in the extracellular loops, as well as the varitint-waddler mutations A419P and I362T and the H283A mutation previously shown to result in constitutive TRPML3 activity. Color-coded *scissors* represent the positions where TRPML3 amino acid sequences were excised to generate TRPML3 mutants with smaller first extracellular loops. *B*, shown are base lines of E361A mutant and wild-type TRPML3-expressing HEK293 cells as well as non-transfected control cells (*NT*) of a representative fura-2 calcium imaging experiment. *C*, effect of the substitution of negatively charged amino acids in the first and second extracellular loops with alanine on $[Ca^{2+}]_i$. Shown are means ± S.E. *Numbers* in *parentheses* indicate the number of experiments. All experiments are means of at least 10–15 cells each. For background subtraction, non-transfected control cells on the same coverslip were used. ***, $p < 0.0001$; **, $p < 0.001$; *, $p < 0.01$ (unpaired Student's *t* test). *D*, TRPML1, TRPML2, and TRPML3 species protein sequence alignment of the region surrounding Glu-361, which is indicated with a *blue arrow*. *Hs*, *Homo sapiens*; *Mm*, *Mus musculus*; *Rn*, *Rattus norvegicus*; *Pt*, *Pan troglodytes*; *Pa*, *Pongo abelii*; *Nl*, *Nomascus leucogenys*; *Mmu*, *Macaca mulatta*; *Cj*, *Callithrix jacchus*; *Bt*, *Bos taurus*; *Ec*, *Equus caballus*; *La*, *Loxodonta africana*; *Cf*, *Canis familiaris*; *Cg*, *Cricetulus griseus*; *Am*, *Ailuropoda melanoleuca*; *Xl*, *Xenopus laevis*.

loop would have an effect on TRPML3 channel activity. On the other hand, we thought we could thus possibly narrow down the number of candidates in the first loop. However, all of these deletion mutants were mislocalized and did not reach the plasma membrane as judged by confocal laser scanning microscopy (data not shown). Thus, we continued with generating single-point mutants. We replaced the negatively charged amino acids individually and analyzed the resulting mutants by calcium imaging and confocal laser scanning microscopy. We found that the TRPML3 mutant isoform E361A, one of the two negatively charged amino acids in the second extracellular loop, showed significantly increased $[Ca^{2+}]_i$ in SBS (Fig. 1, *B* and *C*). The constitutively active TRPML3 mutant isoforms A419P (varitint-waddler mutant isoform Va) and H283A (2, 8–9, 12–14) were used as controls for comparison (Fig. 1*C*).

A

Mutant	PM	$[Ca^{2+}]_i$	Mutant	PM	$[Ca^{2+}]_i$
E92A	+	=	D191A	+/-	=
E93A	+/-	<	E192A	+	>
D108A	-	<	E201A	+	=
D111A	+/-	<	D209A	-	<
D112A	-	<	E217A	-	<
D121A	+/-	<	E234A	-	<
D124A	-	<	D237A	+/-	<
E147A	+	=	D240A	+	<
D173A	+	=	D248A	-	<
D176A	+	>	D261A	+	=
D178A	+/-	<	D263A	+	<
E180A	+	>	E268A	+	<
E182A	+	=	D271A	+	<
E184A	+	=	E361A	+	>>
E189A	+	=	D371A	+/-	=
Wild-type	+	=			

B

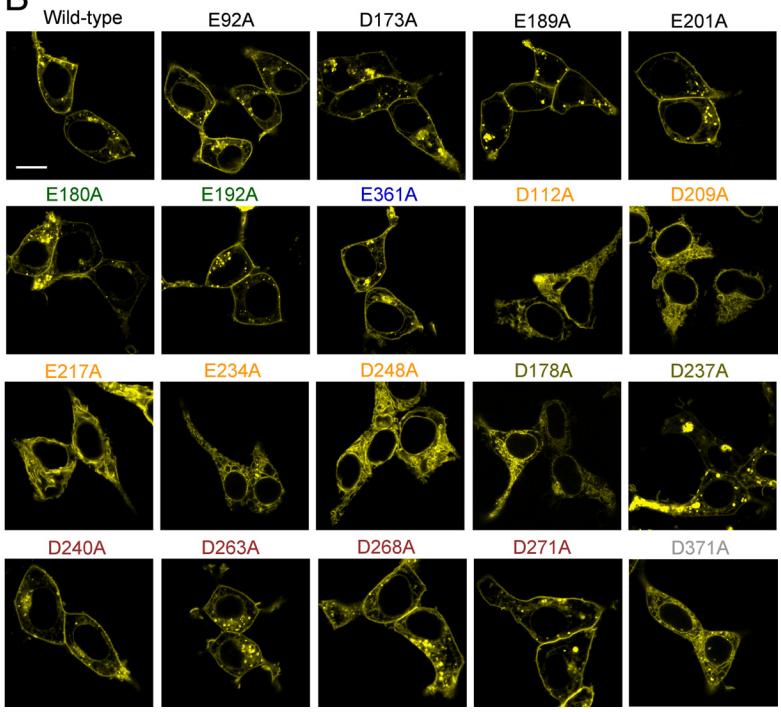

FIGURE 2. **Subcellular localization of TRPML3 loop mutants.** *A*, the table summarizes the laser scanning microscopy and calcium imaging results. *PM*, plasma membrane localization; +, plasma membrane localization comparable with the wild type; +/−, mostly intracellular localization with some potential distribution in the plasma membrane; −, obvious intracellular localization of the channel protein; =, unchanged basal calcium levels compared with the wild-type control; <, >, and ≫, decreased, increased, and strongly increased basal calcium levels in HEK293 cells transfected with the respective mutant isoforms. *B*, subcellular localization of YFP-tagged wild-type TRPML3 and selected mutant isoforms overexpressed in HEK293 cells and analyzed by laser scanning microscopy. *Scale bar* = 10 μm.

Some of the isoforms that carried mutations in the central or putative tip region of the first extracellular loop also showed increased $[Ca^{2+}]_i$ in SBS compared with wild-type TRPML3 (Fig. 1*C*). However, the overall $[Ca^{2+}]_i$ increases were smaller and less significant compared with those in cells expressing either the previously described H283A and A419P mutants or the E361A mutant. Also, amino acid conservation across TRPML2 and TRPML3 species was much lower, *e.g.* in the case of Glu-180 and Glu-192 compared with Glu-361, which is 100% conserved among 30 *TRPML2* and *TRPML3* genes (Fig. 1*D*). Interestingly, the amino acid directly adjacent to Glu-361, Ile-362, is mutated to threonine in varitint-waddler Va^J mutant mice (A419P + I362T) and reportedly causes an amelioration of the Va mutant phenotype (A419P) (3).

Some of the non-responding mutants were clearly mislocalized as judged by laser scanning microscopy, *e.g.* D112A, D209A, and E217A (Fig. 2). However, other mutant isoforms with significantly smaller $[Ca^{2+}]_i$ compared with the wild type, namely D240A, D263A, E268A, and D271A, were still detectable in the plasma membrane (Fig. 2).

Increased Activity of E361A in SBS Revealed by Whole-cell Patch Clamp Measurements—To confirm the above-described calcium imaging results, whole-cell patch clamp experiments were performed. Constitutively active inwardly rectifying currents were recorded in SBS from HEK293 cells expressing E361A. Currents were similar in size to those evoked by LSS in wild-type TRPML3-expressing cells (Fig. 3*A* and Fig. 4, *A* and *B*) (1). As expected, D371A, the other negatively charged amino acid in the same loop, did not display increased constitutive activity. This mutant control channel appeared to localize to the plasma membrane, albeit with low efficacy (Fig. 2), and did not display increased levels of intracellular calcium when tested in SBS (Fig. 1*C*).

When exposing E361A to LSS, we still noted some additional increase in TRPML3 activity (increase in average current densities by ~2-fold *versus* ~5-fold in the wild type) (Fig. 3, *C* and *D*, and Fig. 4, *A* and *B*). Hence, we cannot exclude that additional residues may be involved in extracellular sodium inhibition, but it appears that Glu-361 has a significant impact on the sodium-mediated channel block.

In summary, our mutagenesis screen led to the identification of several mutant TRPML3 isoforms in both the first and second extracellular loops that are constitutively active in SBS. The strongest effect was recorded for the E361A mutant. This observation fits well with previous findings (9–10), suggesting that the two extracellular loops are sensitive to mutations with direct consequences for proton and sodium inhibition.

TRPML2 Activation by LSS—In contrast to TRPML1, which contains both N- and C-terminal dileucine motifs ((D/E)*XXX*L(L/I) motifs) for endolysosomal targeting (16–18) and which is found predominantly in intracellular vesicles, TRPML2 and TRPML3 appear to be present both at the plasma membrane and in intracellular structures, at least in the overexpression system (1, 15, 19, 20). Such dual subcellular location has been suggested before for other TRP channels such as TRPM1, TRPM2, TRPV2, and TRPV5 (21–24).

Here, we observed that TRPML2 also showed increased activity in LSS (Fig. 4, *A* and *B*). This observation suggests that

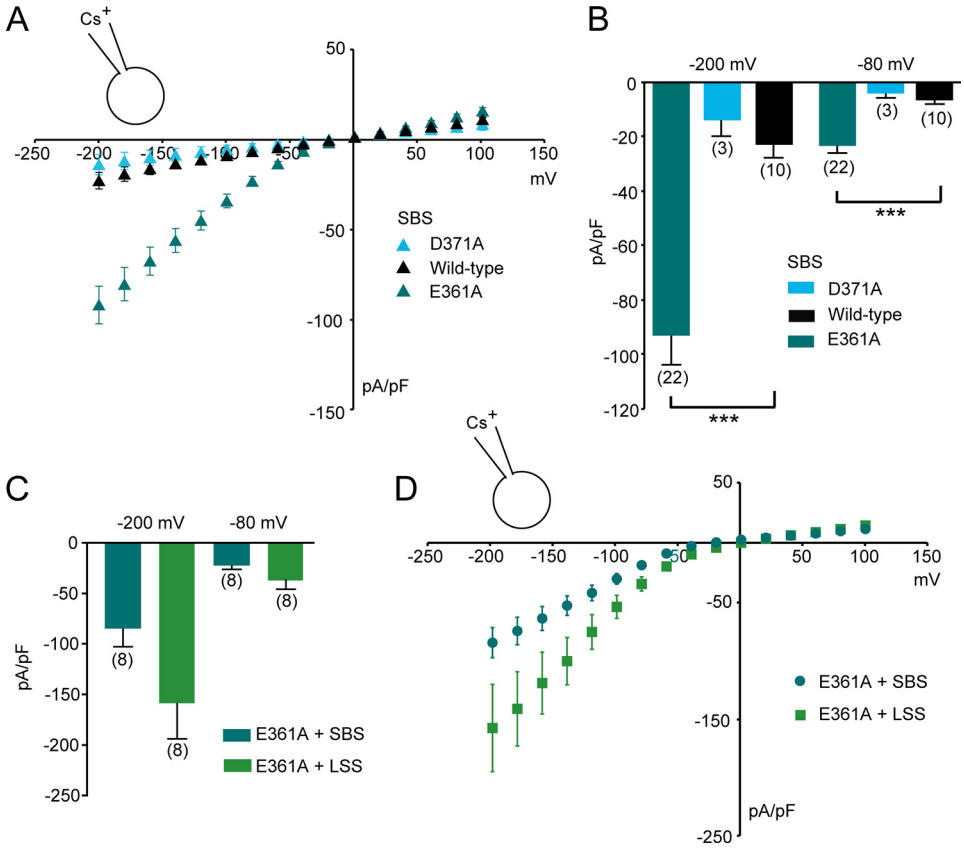

FIGURE 3. **Currents recorded from HEK293 cells expressing TRPML3 loop mutants E361A and D371A.** *A* and *B*, steady-state current-voltage plots of whole-cell currents (*A*) and average inward current densities (*B*) measured in HEK293 cells transfected with the extracellular loop mutants or wild-type TRPML3 in response to 10-ms voltage steps from a holding potential of +10 mV between −200 and +100 mV in 20-mV incremental steps (normalized by cell capacitance (picofarads (*pF*)). Constitutively active inwardly rectifying currents were present in TRPML3(E361A)-expressing cells and were not detectable in TRPML3(D371A)-expressing cells. Shown are means ± S.E. *Numbers* in *parentheses* indicate the number of experiments. ***, $p < 0.0001$ (unpaired Student's *t* test) compared with the wild type. *C* and *D*, average inward current densities (*C*) and steady-state current-voltage plots (*D*) of whole-cell currents at −80 and −200 mV from experiments similar to the ones described for *A* and *B* and normalized to cell capacitance. Shown are means ± S.E. *Numbers* in *parentheses* indicate the number of experiments.

TRPML2 is similar to TRPML3 with respect to permissive activation at low extracellular sodium concentrations. For intracellular compartments, this would mean that TRPML2 is very likely active in extracytosolic fluids that are low in sodium. The electrophysiological recordings also confirmed the subcellular localization of TRPML2 that we observed by confocal microscopy. However, compared with TRPML3, the amount of TRPML2 protein at the plasma membrane appears to be much smaller, possibly explaining the lower response levels of TRPML2 compared with TRPML3 (Fig. 4*C*). TRPML1 did not respond to LSS in whole-cell patch clamp experiments, as was expected from its subcellular localization. In contrast, when coexpressed *in vitro*, TRPML1 appears to tightly regulate the surface expression and functional activity of TRPML2 and TRPML3 channels at the plasma membrane (1, 25–28). This may also hold true for *in vivo* situations when coexpression occurs.

TRPML2 Activation by Small Chemical Compounds Confirms Similarity to TRPML3 and Presence of Functional Channels at Plasma Membrane—To confirm the functional activity of TRPML2 at the plasma membrane, we used the following recently identified small molecule agonists of TRPML3, which had been shown in calcium imaging experiments to also evoke calcium signals in HEK293 cells transfected with TRPML2 (1): SF-21 (4-chloro-*N*-(2-morpholin-4-ylcyclohexyl)benzenesulfonamide), SF-41 (1-(2,4-dimethylphenyl)-4-piperidin-1-ylsulfonylpiperazine), and SF-81 (4,6-dimethyl-3-(2-methylphenyl)sulfonyl-1-propan-2-ylpyridin-2-one).

Whole-cell patch clamp experiments revealed that these three compounds activated TRPML2 significantly compared with YFP-transfected control cells (Fig. 5, *A* and *B*). As a positive control, the TRPML2 equivalent of the constitutively active TRPML3 mutant isoform A419P, TRPML2(A396P), was used (12). TRPML2(A396P) showed similar current densities as wild-type TRPML2 activated with SF-21, SF-41, or SF-81 (Fig. 5, *A*–*C*). As expected from analogous TRPML3 experiments (1), currents obtained with small molecule agonists were significantly larger than those evoked with LSS.

DISCUSSION

Constitutive activity has been demonstrated for a variety of mutant TRPML isoforms. Initially, it was found that the varitint-waddler mutant isoforms of TRPML3 and the equivalent mutant isoforms of TRPML1 and TRPML2 (TRPML1(V432P) or TRPML1 Va and TRPML2(A396P) or TRPML2 Va) display constitutively active large inwardly rectifying currents, leading to rapid cell death *in vitro* and *in vivo* (1, 2, 12–15, 29–33). Due to its presence in the inner ear and in

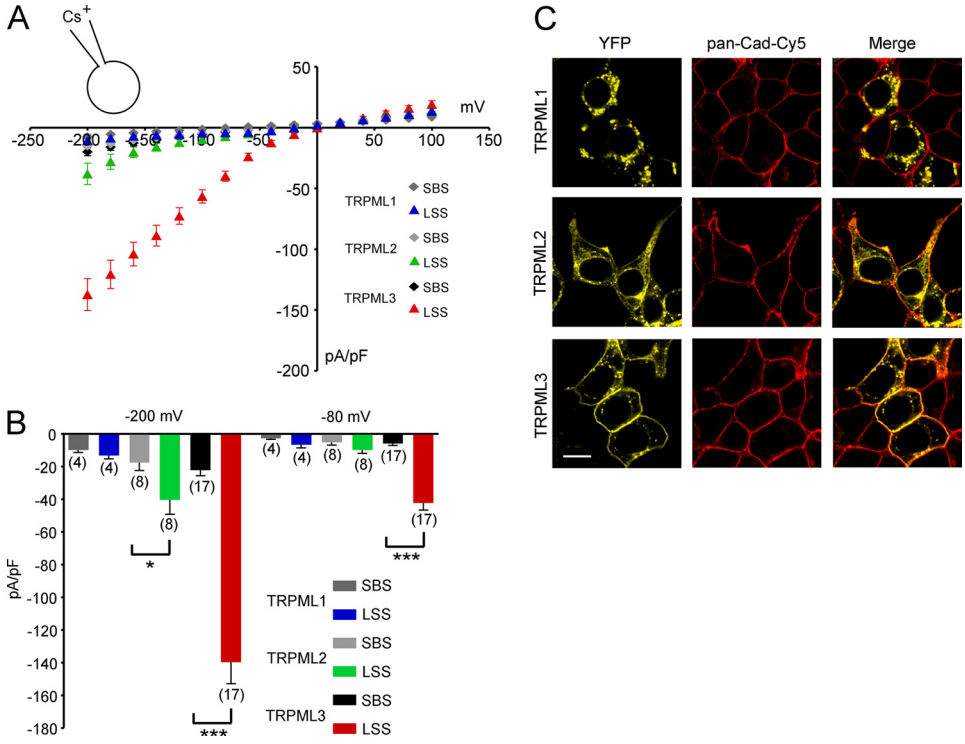

FIGURE 4. **Effect of LSS on HEK293 cells expressing TRPML1, TRPML2, or TRPML3.** *A*, steady-state current-voltage plots of whole-cell currents elicited in HEK293 cells transfected with wild-type TRPML1, TRPML2, or TRPML3 in response to 10-ms voltage steps from a holding potential of +10 mV between −200 and +100 mV in 20-mV incremental steps (normalized by cell capacitance (picofarads (*pF*)). Shown are the currents before and after perfusion with extracellular solution containing 2 mM NaCl, 150 mM KCl, 0.25 mM $CaCl_2$, 10 mM HEPES, and 10 mM D-glucose at pH 7.4 (LSS). The major cation in the pipette solution was 150 mM Cs^+ (pH 7.2). *B*, average inward current densities at −80 and −200 mV from the experiments in *A* and normalized by cell capacitance. Shown are means ± S.E. *Numbers* in *parentheses* indicate the number of experiments. ***, $p < 0.0001$; *, $p < 0.01$ (unpaired Student's *t* test). *C*, expression of the three TRPML channels in HEK293 cells. Shown are representative confocal micrographs of HEK293 cells overexpressing C-terminally YFP-fused constructs of TRPML1, TRPML2, and TRPML3 (*yellow*). Significant amounts of TRPML2 and TRPML3 were associated with the plasma membrane, which is visualized with Cy5-conjugated anti-pan-cadherin antibody (*pan-Cad-Cy5*; *red*; Abcam). *Scale bar* = 10 μm.

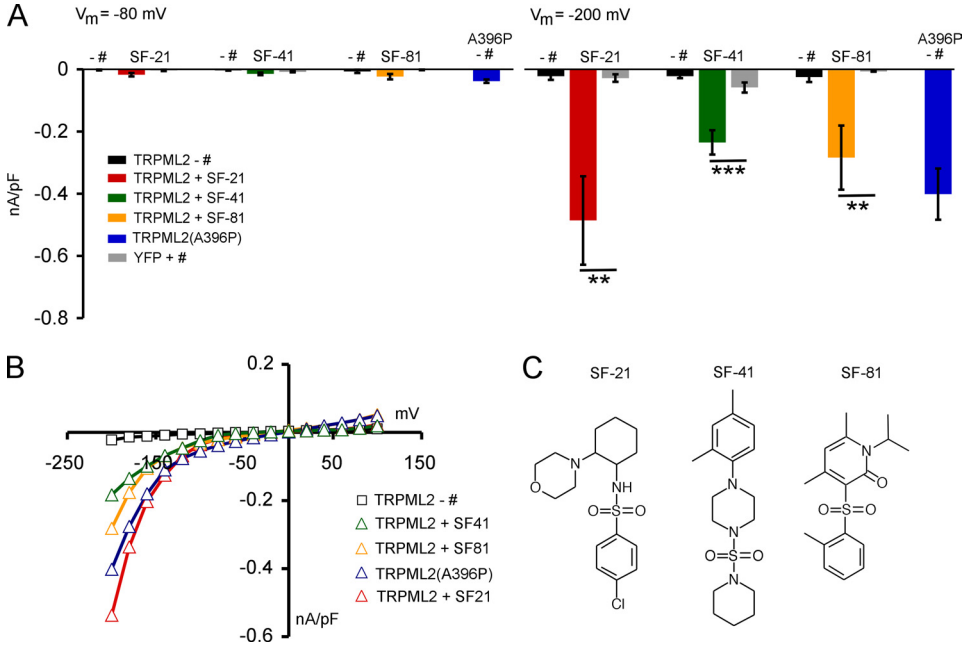

FIGURE 5. **Effect of different chemical stimuli on TRPML2.** *A*, average inward current densities in the presence and absence of different chemical stimuli in SBS from experiments as shown in *B* at −80 and −200 mV and normalized by cell capacitance (picofarads (*pF*)). Shown are means ± S.E. ***, $p < 0.0001$; **, $p < 0.001$ (unpaired Student's *t* test). + #, with compound; − #, without compound. Compounds were used at a final concentration of 10 μM each. *B*, steady-state current-voltage plots of whole-cell currents as summarized for *A* in the presence of different chemical stimuli in SBS. The major cation in the pipette solution was 150 mM Cs^+ (pH 7.2). *C*, chemical formulae of compounds SF-21, SF-41, and SF-81.

melanocytes, mice with the TRPML3 varitint-waddler mutant display a severe auditory and vestibular phenotype as well as significant coat color dilution. For the TRPML3 varitint-waddler mutant isoforms Va and Va^J, it was originally hypothesized that the constitutive activity is caused by a kink, hinge, or swivel in TMD5 due to the exchange of alanine with proline at position 419, leading to a structural change in the channel pore (8, 12). Kim *et al.* (9) have also suggested that, in addition to structural changes in the pore region, the underlying reason for the constitutive activity of Va and Va^J isoforms may be due, at least in part, to the disruption of the regulation of TRPML3 by extracytosolic (luminal) H^+ that locks the channel in an open state. They demonstrated that certain histidines in the extracellular loop of TRPML3, notably His-252, His-273, and His-283, are responsible for TRPML3 regulation by extracytosolic H^+. Based on these findings, it was suggested that the extracytosolic H^+ regulatory domain influences the orientation of TMD5 and that binding of extracytosolic H^+ to His-283 exerts a long-range conformational change that affects pore opening (9).

A419P (Va) and H283A are both insensitive to changes in extracellular sodium. Here, we have shown that the open probability of the TRPML3 channel in high extracellular sodium is also increased, albeit less strongly, when Glu-361 in the second extracellular loop is mutated to alanine. As mentioned above, the amino acid directly adjacent to Glu-361, Ile-362, which is mutated in Va^J mice (A419P + I362T), causes an amelioration of the Va phenotype (A419P). If Glu-361 has an impact on the open probability of TRPML3 in high extracellular sodium, Ile-362 may directly interfere with the underlying mechanism when likewise mutated, *e.g.* by a conformational change. Alternatively, if Glu-361 directly affects sodium binding, an exchange of the neutral amino acid isoleucine with the nucleophilic threonine next to Glu-361 may potentially enhance sodium binding and thus decrease the A419P mutant channel activity, leading to the observed rescue effect (3).

Furthermore, it cannot be excluded that other monovalent ions are also inhibiting TRPML3 activity, with Na^+ being the most potent inhibitor, whereas Cs^+, K^+, and Li^+, for example, are less potent due to decreased binding affinity for the monovalent binding site. This would explain why the E361A mutant activity in SBS can still be increased with LSS. E361A would bind Na^+ with decreased affinity, but the binding affinities for K^+ and Li^+ would be even further decreased. Thus, TRPML3 could generally act as a monovalent sensor.

A functional interaction between distinct residues in the first and second extracellular loops or the pore loop, which would require low extracellular pH and/or high extracellular sodium, may be an interesting scenario. The pore loop contains four negatively charged amino acids. For three of these, mutational effects have been described before, namely Glu-449, Asp-458, and Asp-459 (10). Glu-449 is predicted to be in the pore helix, whereas Asp-458 and Asp-459 are predicted to line the selectivity filter. Whereas mutation of Asp-458 to Lys, Ala, or Asn results in an inactive channel, the E449A mutation renders the channel constitutively active (10). Thus, amino acids in the two extracellular loops, as well as in the pore loop, can render TRPML3 constitutively active when mutated. Among the 20 amino acids, at least 12 (especially charged amino acids: Asp, Glu, Arg, and Lys) can form hydrogen bonds with their side chains. Hydrogen bonds (*e.g.* between His-Glu or His-Asp) are a common element in many catalytic sites (34, 35). Gao *et al.* (36) showed, in site-directed mutagenesis studies, that the closely linked residues Glu-13 and His-278 in A_{2A} adenosine receptors are involved in ligand binding and sodium modulation. As in a channel selectivity filter, proper geometry and energetics may play an important role in precisely positioning the two extracellular loop(s) and thus blocking the TRPML3 pore entrance.

The identified small molecule activators of TRPML2 and TRPML3 could act in a similar manner by disrupting the interaction between the two extracellular loops or between the first extracellular loop and the pore loop (or both) and may thus lock the channel in an open state. Many of the TRPML3 small molecule agonists are sulfonamides, and sulfonamides are among the chemical groups capable of forming hydrogen bonds with several amino acids (37), thus enabling them to interfere with potential amino acid interactions in TRPML2 or TRPML3.

It should be noted that although TRPML1 has not been further investigated here, it has been demonstrated recently, with the whole-lysosome patch clamp technique, as well as with calcium imaging using a plasma membrane variant of TRPML1, TRPML1(NC), which lacks the N- and C-terminal dileucine motifs, that TRPML1 can likewise be activated by some of the recently identified TRPML3 agonists (1). In addition, all TRPML channels can be activated by the endogenous compound $PI(3,5)P_2$ (1, 38–41). This points to common activation mechanism(s) for all three TRPML channels, at least with regard to some of the identified small chemical activators and $PI(3,5)P_2$ (41).

Acknowledgments—We thank Dr. Martin Biel (Ludwig-Maximilians-Universität München) for kindly reading and commenting on the manuscript and Dr. Anthony J. Ricci and Michael Schnee (Stanford University) for technical support.

REFERENCES

1. Grimm, C., Jörs, S., Saldanha, S. A., Obukhov, A. G., Pan, B., Oshima, K., Cuajungco, M. P., Chase, P., Hodder, P., and Heller, S. (2010) Small molecule activators of TRPML3. *Chem. Biol.* **17,** 135–148
2. Nagata, K., Zheng, L., Madathany, T., Castiglioni, A. J., Bartles, J. R., and García-Añoveros, J. (2008) The varitint-waddler (Va) deafness mutation in TRPML3 generates constitutive, inward rectifying currents and causes cell degeneration. *Proc. Natl. Acad. Sci. U.S.A.* **105,** 353–358
3. Di Palma, F., Belyantseva, I. A., Kim, H. J., Vogt, T. F., Kachar, B., and Noben-Trauth, K. (2002) Mutations in *Mcoln3* associated with deafness and pigmentation defects in varitint-waddler (Va) mice. *Proc. Natl. Acad. Sci. U.S.A.* **99,** 14994–14999
4. van Aken, A. F., Atiba-Davies, M., Marcotti, W., Goodyear, R. J., Bryant, J. E., Richardson, G. P., Noben-Trauth, K., and Kros, C. J. (2008) TRPML3 mutations cause impaired mechano-electrical transduction and depolarization by an inward-rectifier cation current in auditory hair cells of varitint-waddler mice. *J. Physiol.* **586,** 5403–5418
5. Takumida, M., and Anniko, M. (2010) Expression of transient receptor potential channel mucolipin (TRPML) and polycystine (TRPP) in the mouse inner ear. *Acta Otolaryngol.* **130,** 196–203
6. Castiglioni, A. J., Remis, N. N., Flores, E. N., and García-Añoveros, J. (2011) Expression and vesicular localization of mouse *Trpml3* in stria vascularis, hair cells, and vomeronasal and olfactory receptor neurons. *J. Comp. Neurol.* **519,** 1095–1114

7. Noben-Trauth, K. (2011) The TRPML3 channel: from gene to function. *Adv. Exp. Med. Biol.* **704,** 229–237
8. Kim, H. J., Li, Q., Tjon-Kon-Sang, S., So, I., Kiselyov, K., and Muallem, S. (2007) Gain-of-function mutation in TRPML3 causes the mouse varitint-waddler phenotype. *J. Biol. Chem.* **282,** 36138–36142
9. Kim, H. J., Li, Q., Tjon-Kon-Sang, S., So, I., Kiselyov, K., Soyombo, A. A., and Muallem, S. (2008). A novel mode of TRPML3 regulation by extracytosolic pH absent in the varitint-waddler phenotype. *EMBO J.* **27,** 1197–1205
10. Kim, H. J., Yamaguchi, S., Li, Q., So, I., and Muallem, S. (2010) Properties of the TRPML3 channel pore and its stable expansion by the varitint-waddler-causing mutation. *J. Biol. Chem.* **285,** 16513–16520
11. Yamaguchi, S., and Muallem, S. (2010) Opening the TRPML gates. *Chem. Biol.* **17,** 209–210
12. Grimm, C., Cuajungco, M. P., van Aken, A. F., Schnee, M., Jörs, S., Kros, C. J., Ricci, A. J., and Heller, S. (2007) A helix-breaking mutation in TRPML3 leads to constitutive activity underlying deafness in the varitint-waddler mouse. *Proc. Natl. Acad. Sci. U.S.A.* **104,** 19583–19588
13. Grimm, C., Jörs, S., and Heller, S. (2009) Life and death of sensory hair cells expressing constitutively active TRPML3. *J. Biol. Chem.* **284,** 13823–13831
14. Xu, H., Delling, M., Li, L., Dong, X., and Clapham, D. E. (2007) Activating mutation in a mucolipin transient receptor potential channel leads to melanocyte loss in varitint-waddler mice. *Proc. Natl. Acad. Sci. U.S.A.* **104,** 18321–18326
15. Lev, S., Zeevi, D. A., Frumkin, A., Offen-Glasner, V., Bach, G., and Minke, B. (2010) Constitutive activity of the human TRPML2 channel induces cell degeneration. *J. Biol. Chem.* **285,** 2771–2782
16. Mattera, R., Boehm, M., Chaudhuri, R., Prabhu, Y., and Bonifacino, J. S. (2011) Conservation and diversification of dileucine signal recognition by adaptor protein (AP) complex variants. *J. Biol. Chem.* **286,** 2022–2030
17. Steenhuis, P., Herder, S., Gelis, S., Braulke, T., and Storch, S. (2010) Lysosomal targeting of the CLN7 membrane glycoprotein and transport via the plasma membrane require a dileucine motif. *Traffic* **11,** 987–1000
18. Vergarajauregui, S., and Puertollano, R. (2006) Two dileucine motifs regulate trafficking of mucolipin-1 to lysosomes. *Traffic* **7,** 337–353
19. Karacsonyi, C., Miguel, A. S., and Puertollano, R. (2007) Mucolipin-2 localizes to the Arf6-associated pathway and regulates recycling of GPI-APs. *Traffic* **8,** 1404–1414
20. Flores, E. N., and García-Añoveros, J. (2011) TRPML2 and the evolution of mucolipins. *Adv. Exp. Med. Biol.* **704,** 221–228
21. Patel, S., and Docampo, R. (2009) In with the TRP channels: intracellular functions for TRPM1 and TRPM2. *Sci. Signal.* **2,** pe69
22. Abe, K., and Puertollano, R. (2011) Role of TRP channels in the regulation of the endosomal pathway. *Physiology* **26,** 14–22
23. Gees, M., Colsoul, B., and Nilius, B. (2010) The role of transient receptor potential cation channels in Ca^{2+} signaling. *Cold Spring Harb. Perspect. Biol.* **2,** a003962
24. Dong, X. P., Wang, X., and Xu, H. (2010) TRP channels of intracellular membranes. *J. Neurochem.* **113,** 313–328
25. Zeevi, D. A., Lev, S., Frumkin, A., Minke, B., and Bach, G. (2010) Heteromultimeric TRPML channel assemblies play a crucial role in the regulation of cell viability models and starvation-induced autophagy. *J. Cell Sci.* **123,** 3112–3124
26. Curcio-Morelli, C., Zhang, P., Venugopal, B., Charles, F. A., Browning, M. F., Cantiello, H. F., and Slaugenhaupt, S. A. (2010) Functional multimerization of mucolipin channel proteins. *J. Cell Physiol.* **222,** 328–335
27. Venkatachalam, K., Hofmann, T., and Montell, C. (2006) Lysosomal localization of TRPML3 depends on TRPML2 and the mucolipidosis-associated protein TRPML1. *J. Biol. Chem.* **281,** 17517–17527
28. Bach, G., Zeevi, D. A., Frumkin, A., and Kogot-Levin, A. (2010) Mucolipidosis type IV and the mucolipins. *Biochem. Soc. Trans.* **38,** 1432–1435
29. Dong, X. P., Wang, X., Shen, D., Chen, S., Liu, M., Wang, Y., Mills, E., Cheng, X., Delling, M., and Xu, H. (2009) Activating mutations of the TRPML1 channel revealed by proline-scanning mutagenesis. *J. Biol. Chem.* **284,** 32040–32052
30. Cheng, X., Shen, D., Samie, M., and Xu, H. (2010) Mucolipins: intracellular TRPML1–3 channels. *FEBS Lett.* **584,** 2013–2021
31. Lev, S., and Minke, B. (2010) Constitutive activity of TRP channel: methods for measuring the activity and its outcome. *Methods Enzymol.* **484,** 591–612
32. Samie, M. A., Grimm, C., Evans, J. A., Curcio-Morelli, C., Heller, S., Slaugenhaupt, S. A., and Cuajungco, M. P. (2009) The tissue-specific expression of *TRPML2* (*Mcoln-2*) gene is influenced by the presence of TRPML1. *Eur. J. Physiol.* **459,** 79–91
33. Puertollano, R., and Kiselyov, K. (2009) TRPMLs: in sickness and in health. *Am. J. Physiol. Renal. Physiol.* **296,** F1245–F1254
34. Lau, E. Y., and Bruice, T. C. (1999) Consequences of breaking the Asp-His hydrogen bond of the catalytic triad: effects on the structure and dynamics of the serine esterase cutinase. *Biophys. J.* **77,** 85–98
35. Tanaka, M., Ishimori, K., and Morishima, I. (1998) Structural roles of the highly conserved Glu residue in the heme distal site of peroxidases. *Biochemistry* **37,** 2629–2638
36. Gao, Z. G., Jiang, Q., Jacobson, K. A., and Ijzerman, A. P. (2000) Site-directed mutagenesis studies of human A_{2A} adenosine receptors: involvement of Glu-13 and His-278 in ligand binding and sodium modulation. *Biochem. Pharmacol.* **60,** 661–668
37. Chan, A. W., Laskowski, R. A., and Selwood, D. L. (2010) Chemical fragments that hydrogen bond to Asp, Glu, Arg, and His side chains in protein-binding sites. *J. Med. Chem.* **53,** 3086–3094
38. Dong, X. P., Shen, D., Wang, X., Dawson, T., Li, X., Zhang, Q., Cheng, X., Zhang, Y., Weisman, L. S., Delling, M., and Xu, H. (2010) $PI(3,5)P_2$ controls membrane trafficking by direct activation of mucolipin Ca^{2+} release channels in the endolysosome. *Nat. Commun.* **1,** 38
39. Shen, D., Wang, X., Li, X., Zhang, X., Yao, Z., Dibble, S., Dong, X. P., Yu, T., Lieberman, A. P., Showalter, H. D., and Xu, H. (2012) Lipid storage disorders block lysosomal trafficking by inhibiting a TRP channel and lysosomal calcium release. *Nat. Commun.* **3,** 731
40. Saldanha, S. A., Grimm, C., Mercer, B. A. Choi, J. Y., Allais, C., Roush, W. R., Heller, S., and Hodder, P. (2011) Campaign to identify agonists of transient receptor potential channels 3 and 2 (TRPML3 &TRPML2). *Probe Reports from the NIH Molecular Libraries Program*, National Center for Biotechnology Information, Bethesda, MD (November 13, 2009; updated May 5, 2011)
41. Grimm, C., Hassan, S., Wahl-Schott, C., and Biel, M. (2012) TRPML and two-pore channels in endolysosomal cation homeostasis. *J. Pharmacol. Exp. Ther.* 10.1124/jpet.112.192880